

## Synthesis, antitumor activity and QSAR studies of some 4-aminomethylidene derivatives of edaravone

Violeta Marković<sup>a</sup>, Slavica Erić<sup>b</sup>, Zorica D. Juranić<sup>c</sup>, Tatjana Stanojković<sup>c</sup>, Ljubinka Joksović<sup>a</sup>, Branislav Ranković<sup>d</sup>, Marijana Kosanić<sup>d</sup>, Milan D. Joksović<sup>a,\*</sup>

<sup>a</sup> Faculty of Sciences, Department of Chemistry, University of Kragujevac, R. Domanovica 12, 34000 Kragujevac, Serbia

<sup>b</sup> Faculty of Pharmacy, University of Belgrade, Vojvode Stepe 450, 11000 Belgrade, Serbia

<sup>c</sup> Institute of Oncology and Radiology of Serbia, Pasterova 14, 11000 Belgrade, Serbia

<sup>d</sup> Faculty of Sciences, Department of Biology, University of Kragujevac, R. Domanovica 12, 34000 Kragujevac, Serbia

### ARTICLE INFO

#### Article history:

Received 1 September 2010

Available online 28 October 2010

#### Keywords:

Edaravone derivatives

Antitumor activity

QSAR studies

### ABSTRACT

A series of aminomethylidene derivatives obtained from 4-formylederavone were synthesized and characterized by IR, NMR and elemental analysis. All the compounds were screened for their antitumor activity. The compound containing 5-phenylpyrazole moiety (**3q**) exhibited remarkable antitumor activity in *in vitro* assays, especially against human breast cancer MDA-MB-361 and MDA-MB-453 cell lines. The most important whole-molecule descriptors for antitumor activity on MDA-MB-453 cells belong to the group of quantum-chemical descriptors.

© 2010 Elsevier Inc. All rights reserved.

### 1. Introduction

The increasing interest in biological studies of pyrazol-5-ones in the last decade is a consequence of their wide use as the pharmaceutically important class of compounds. Among them, edaravone (3-methyl-1-phenyl-2-pyrazolin-5-one, Radicut<sup>®</sup>, Mitsubishi Tanabe Pharma Corporation) represents an example of one of the prominent drugs which acts as a potent cerebral neuroprotectant that readily scavenges reactive oxygen species and inhibits proinflammatory responses after brain ischemia in the treatment of patients in the acute stage of cerebral infarction [1,2].

Unlike edaravone, its derivatives synthesized by functionalization of the C4 position of pyrazol-5-one ring have been reported to provide a diversity of synthetic and pharmacological possibilities as pyrazol-5-one is the core structure of numerous biologically active heterocycles. Knoevenagel–Michael reaction of two equivalents of edaravone with various aromatic aldehydes afforded 4,4'-(arylmethylene)bis(1H-pyrazol-5-ols) (**I**, Fig. 1) with excellent activity against peste des petits ruminant virus (PPRV) [3]. Condensation of edaravone with pyrimidine nucleoside resulted in generation of the novel 5-substituted pyrimidine nucleosides (**II**, Fig. 1) with potent *in vitro* antiviral activity against representative orthopoxviruses [4]. Several rigid edaravone derivatives (**III**, Fig. 1) were recently synthesized by condensation of 4-formylederavone with

secondary amines and evaluated as inhibitors of *Mycobacterium tuberculosis*, the causative agent of tuberculosis [5].

The derivatives of pyrazol-5-one have already been discovered as antitumor agents. For example, thiadiazole substituted pyrazol-5-ones (**IV**, Fig. 1) were identified as potent KDR kinase inhibitors in regulating angiogenesis which is crucial for the proliferation of tumor cells [6]. It has also been discovered that edaravone itself enhances the antitumor effects of CPT-11 in murine colon cancer by increasing apoptosis [7] and also reacts with a pterin derivative to produce a cytotoxic substance that induces intracellular reactive oxygen species generation and cell death [8]. A new derivative of edaravone, 4,4-dichloro-1-(2,4-dichlorophenyl)-3-methylpyrazol-5-one (**V**, Fig. 1), was identified as a potent blocker of human telomerase and is considered to be a valuable substance for medical treatment of cancer and related diseases [9]. In spite of widely surveyed pharmacological action of series of edaravone derivatives, antitumor screening of compounds obtained by condensation of 4-formylederavone with primary amines has not been so far reported. The particular attention in this work is focused on introduction of the known antitumor 3-aminopyrazole pharmacophores [10,11] at C4 position of the edaravone moiety and their *in vitro* antitumor evaluation.

However, the mechanism of antitumor action of edaravone derivatives synthesized in this work, containing pyrazol-5-one as a core, has not been rationalized yet. Thus, we have performed quantitative structure–cellular activity relationships study in order to investigate the structural features of edaravone analogs that may be important for antitumor activity and therefore to get some

\* Corresponding author.

E-mail address: [mjoksovic@kg.ac.rs](mailto:mjoksovic@kg.ac.rs) (M.D. Joksović).

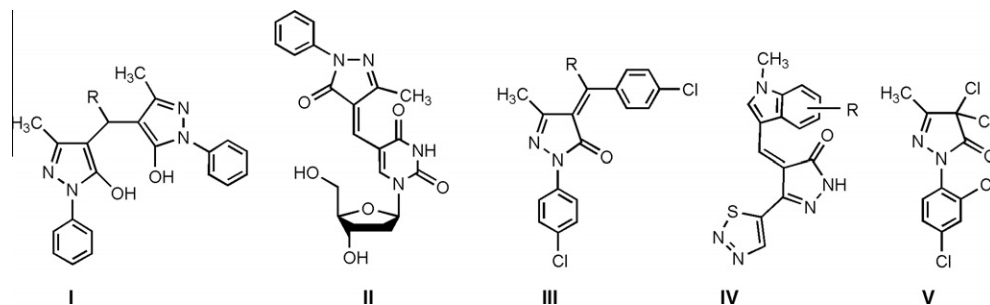


Fig. 1. Some pyrazol-5-one derivatives with pronounced biological activity.

basic direction for further investigation of the mechanism of action and optimization of these compounds.

## 2. Experimental

### 2.1. Physical measurements

Melting points were determined on a Mel-Temp capillary melting points apparatus, model 1001 and are uncorrected. Elemental (C, H, N, S) analysis of the samples was carried out by standard micromethods in the Center for Instrumental Analysis, Faculty of Chemistry, Belgrade. IR spectra were recorded on a Perkin Elmer Spectrum One FT-IR spectrometer with a KBr disc. All  $^1\text{H}$  and  $^{13}\text{C}$  NMR spectra were recorded on a Varian Gemini 200 spectrometer.

### 2.2. General procedure for the preparation of 3a–q

A mixture of 4-formyl-3-methyl-1-phenyl-2-pyrazolin-5-one (**2**, 0.303 g, 1.5 mmol), primary amine (3 mmol) and *p*-toluenesulfonic acid monohydrate (0.011 g, 0.06 mmol) in ethanol (10 mL) was heated to reflux for 2 h. After cooling, the precipitate was filtered off, washed with a little cold ethanol and dried in vacuo over anhydrous  $\text{CaCl}_2$ .

#### 2.2.1. 3-Methyl-4-[[2-methylphenyl]amino]methylidene]-1-phenyl-4,5-dihydro-1H-pyrazol-5-one (3a)

0.39 g (89%); yellow powder; Mp = 182–183 °C.  $^1\text{H}$  NMR (200 MHz,  $\text{DMSO-d}_6$ ):  $\delta$  = 2.29 (s, 3H,  $\text{CH}_3$ ), 2.37 (s, 3H,  $\text{CH}_3$ ), 7.10–7.18 (m, 2H, Ar–H), 7.30–7.44 (m, 4H, Ar–H), 7.74 (d, 1H,  $J$  = 8.2 Hz, Ar–H), 8.00 (dd, 2H,  $J$  = 7.4 and 1.2 Hz, Ar–H), 8.75 (d, 1H,  $J$  = 12.4 Hz, =CH–N), 11.62 (d, 1H,  $J$  = 12.4 Hz, NH).  $^{13}\text{C}$  NMR (50 MHz,  $\text{DMSO-d}_6$ ):  $\delta$  = 12.68, 16.93, 102.36, 115.99, 117.98, 124.08, 125.51, 127.09, 127.56, 128.98, 131.35, 137.15, 139.19, 146.24, 148.99, 165.67. IR (KBr disc,  $\text{cm}^{-1}$ ): 3435, 1667, 1628, 1596, 1551, 1492, 1285, 750. Anal. Calcd for  $\text{C}_{18}\text{H}_{17}\text{N}_3\text{O}$  (291.35 g/mol): C, 74.20; H, 5.88; N, 14.42. Found: C, 74.70; H, 5.93; N, 14.41.

#### 2.2.2. 3-Methyl-4-[[3-methylphenyl]amino]methylidene]-1-phenyl-4,5-dihydro-1H-pyrazol-5-one (3b)

0.35 g (80%); yellow powder; Mp = 103–104 °C (dec).  $^1\text{H}$  NMR (200 MHz,  $\text{DMSO-d}_6$ ):  $\delta$  = 2.29 (s, 3H,  $\text{CH}_3$ ), 2.34 (s, 3H,  $\text{CH}_3$ ), 7.03–7.05 (m, 1H, Ar–H), 7.13 (t, 1H,  $J$  = 7.4 Hz, Ar–H), 7.31–7.40 (m, 5H, Ar–H), 7.99 (dd, 2H,  $J$  = 7.4 and 1.2 Hz, Ar–H), 8.59 (d, 1H,  $J$  = 9.0 Hz, =CH–N), 11.25 (d, 1H,  $J$  = 9.0 Hz, NH).  $^{13}\text{C}$  NMR (50 MHz,  $\text{DMSO-d}_6$ ):  $\delta$  = 12.72, 21.08, 101.94, 115.20, 117.86, 118.22, 123.97, 126.32, 128.98, 129.73, 138.81, 139.29, 139.61, 145.89, 149.21, 165.20. IR (KBr disc,  $\text{cm}^{-1}$ ): 3436, 1664, 1628, 1602, 1545, 1493, 1301, 755. Anal. Calcd for  $\text{C}_{18}\text{H}_{17}\text{N}_3\text{O}$  (291.35 g/mol): C, 74.20; H, 5.88; N, 14.42. Found: C, 74.59; H, 5.84; N, 14.39.

#### 2.2.3. 3-Methyl-4-[[4-methylphenyl]amino]methylidene]-1-phenyl-4,5-dihydro-1H-pyrazol-5-one (3c)

0.35 g (80%); yellow powder; Mp = 165–166 °C.  $^1\text{H}$  NMR (200 MHz,  $\text{DMSO-d}_6$ ):  $\delta$  = 2.28 (s, 3H,  $\text{CH}_3$ ), 2.30 (s, 3H,  $\text{CH}_3$ ), 7.13 (t, 1H,  $J$  = 7.4 Hz, Ar–H), 7.25 (d, 2H,  $J$  = 8.2 Hz, Ar–H), 7.35–7.49 (m, 4H, Ar–H), 8.00 (dd, 2H,  $J$  = 7.4 and 1.2 Hz, Ar–H), 8.56 (d, 1H,  $J$  = 10.8 Hz, =CH–N), 11.31 (d, 1H,  $J$  = 10.8 Hz, NH).  $^{13}\text{C}$  NMR (50 MHz,  $\text{DMSO-d}_6$ ):  $\delta$  = 12.70, 20.51, 101.66, 117.83, 117.95, 123.92, 128.96, 130.29, 135.02, 136.56, 139.34, 145.93, 149.16, 165.17. IR (KBr disc,  $\text{cm}^{-1}$ ): 3437, 1670, 1652, 1593, 1486, 1293, 1284, 754. Anal. Calcd for  $\text{C}_{18}\text{H}_{17}\text{N}_3\text{O}$  (291.35 g/mol): C, 74.20; H, 5.88; N, 14.42. Found: C, 74.49; H, 5.87; N, 14.40.

#### 2.2.4. 3-Methyl-4-[[2-nitrophenyl]amino]methylidene]-1-phenyl-4,5-dihydro-1H-pyrazol-5-one (3d)

0.43 g (89%); orange powder; Mp = 238–239 °C (dec).  $^1\text{H}$  NMR (200 MHz,  $\text{DMSO-d}_6$ ):  $\delta$  = 2.31 (s, 3H,  $\text{CH}_3$ ), 7.15 (t, 1H,  $J$  = 7.4 Hz, Ar–H), 7.35–7.46 (m, 3H, Ar–H), 7.87 (td, 1H,  $J$  = 7.4 and 1.4 Hz, Ar–H), 7.97 (dd, 2H,  $J$  = 7.4 and 1.2 Hz, Ar–H), 8.16 (d, 1H,  $J$  = 8.0 Hz, Ar–H), 8.27 (dd, 1H,  $J$  = 8.2 and 1.2 Hz, Ar–H), 8.71 (d, 1H,  $J$  = 8.4 Hz, =CH–N), 12.68 (d, 1H,  $J$  = 8.4 Hz, NH).  $^{13}\text{C}$  NMR (50 MHz,  $\text{DMSO-d}_6$ ):  $\delta$  = 12.18, 105.58, 117.92, 118.67, 124.24, 124.87, 126.47, 129.04, 135.09, 136.29, 137.16, 138.91, 144.20, 149.51, 164.61. IR (KBr disc,  $\text{cm}^{-1}$ ): 3436, 1672, 1624, 1599, 1331, 1306, 1257, 1161, 747. Anal. Calcd for  $\text{C}_{17}\text{H}_{14}\text{N}_4\text{O}_3$  (322.32 g/mol): C, 63.35; H, 4.38; N, 17.38. Found: C, 63.32; H, 4.38; N, 17.40.

#### 2.2.5. 3-Methyl-4-[[3-nitrophenyl]amino]methylidene]-1-phenyl-4,5-dihydro-1H-pyrazol-5-one (3e)

0.46 g (95%); light orange powder; Mp = 181–182 °C (dec).  $^1\text{H}$  NMR (200 MHz,  $\text{DMSO-d}_6$ ):  $\delta$  = 2.29 (s, 3H,  $\text{CH}_3$ ), 7.13 (t, 1H,  $J$  = 7.4 Hz, Ar–H), 7.40 (t, 2H,  $J$  = 8.0 Hz, Ar–H), 7.67 (t, 1H,  $J$  = 8.0 Hz, Ar–H), 7.97 (m, 4H, Ar–H), 8.52 (t, 1H,  $J$  = 2.2 Hz, Ar–H), 8.64 (bs, 1H, =CH–N), 11.36 (bs, 1H, NH).  $^{13}\text{C}$  NMR (50 MHz,  $\text{DMSO-d}_6$ ):  $\delta$  = 12.81, 103.36, 112.61, 117.82, 119.55, 124.05, 124.69, 128.98, 131.02, 139.14, 140.58, 145.69, 148.97, 149.52, 164.83. IR (KBr disc,  $\text{cm}^{-1}$ ): 3435, 1671, 1643, 1597, 1530, 1502, 1355, 1313, 1292, 738. Anal. Calcd for  $\text{C}_{17}\text{H}_{14}\text{N}_4\text{O}_3$  (322.32 g/mol): C, 63.35; H, 4.38; N, 17.38. Found: C, 63.41; H, 4.40; N, 17.43.

#### 2.2.6. 3-Methyl-4-[[4-nitrophenyl]amino]methylidene]-1-phenyl-4,5-dihydro-1H-pyrazol-5-one (3f)

0.43 g (89%); brown powder; Mp = 204–205 °C (dec).  $^1\text{H}$  NMR (200 MHz,  $\text{DMSO-d}_6$ ):  $\delta$  = 2.30 (s, 3H,  $\text{CH}_3$ ), 7.15 (t, 1H,  $J$  = 7.4 Hz, Ar–H), 7.42 (t, 2H,  $J$  = 7.4 Hz, Ar–H), 7.82 (d, 2H,  $J$  = 9.2 Hz, Ar–H), 7.97 (dd, 2H,  $J$  = 7.4 and 1.2 Hz, Ar–H), 8.29 (d, 2H,  $J$  = 9.2 Hz, Ar–H), 8.64 (bs, 1H, =CH–N), 11.41 (bs, 1H, NH).  $^{13}\text{C}$  NMR (50 MHz,  $\text{DMSO-d}_6$ ):  $\delta$  = 12.78, 104.46, 117.89, 118.26, 124.24, 125.59, 129.05, 132.89, 138.98, 143.92, 144.90, 149.62, 164.74. IR (KBr disc,  $\text{cm}^{-1}$ ): 3421, 1664, 1636, 1591, 1509, 1498, 1339,

1279, 749. Anal. Calcd for  $C_{17}H_{14}N_4O_3$  (322.32 g/mol): C, 63.35; H, 4.38; N, 17.38. Found: C, 63.66; H, 4.39; N, 17.43.

2.2.7. 4-[[4-Hydroxyphenyl]amino]methylidene]-3-methyl-1-phenyl-4,5-dihydro-1H-pyrazol-5-one (**3g**)

0.38 g (86%); yellow powder; Mp = 277–278 °C.  $^1H$  NMR (200 MHz, DMSO- $d_6$ ): 2.26 (s, 3H,  $CH_3$ ), 6.83 (d, 2H,  $J = 9.0$  Hz, Ar–H), 7.11 (t, 1H,  $J = 7.4$  Hz, Ar–H), 7.35–7.43 (m, 4H, Ar–H), 8.00 (dd, 2H,  $J = 7.4$  and 1.2 Hz, Ar–H), 8.45 (bs, 1H, =CH–N), 9.62 (s, 1H, OH), 11.36 (bs, 1H, NH).  $^{13}C$  NMR (50 MHz, DMSO- $d_6$ ):  $\delta = 12.69, 100.93, 116.29, 117.80, 119.77, 123.83, 128.96, 130.88, 139.47, 146.18, 149.01, 155.80, 165.20$ . IR (KBr disc,  $cm^{-1}$ ): 3411, 1665, 1650, 1596, 1522, 1485, 1306, 1267, 752. Anal. Calcd for  $C_{17}H_{15}N_3O_2$  (293.33 g/mol): C, 69.61; H, 5.15; N, 14.33. Found: C, 69.94; H, 5.19; N, 14.38.

2.2.8. 3-Methyl-1-phenyl-4-[[thiophen-2-ylmethyl]amino]methylidene]-4,5-dihydro-1H-pyrazol-5-one (**3h**)

0.28 g (62%); light yellow crystals; Mp = 116–117 °C.  $^1H$  NMR (200 MHz, DMSO- $d_6$ ):  $\delta = 2.17$  (s, 3H,  $CH_3$ ), 4.83 (s, 2H,  $CH_2$ ), 7.02–7.16 (m, 3H, 2H(Thi) and 1H(Ar)), 7.32 (t, 2H,  $J = 7.4$  Hz, Ar–H), 7.52 (dd, 1H,  $J = 5.2$  and 1.2 Hz, Thi–H), 7.96 (dd, 2H,  $J = 7.4$  and 1.2 Hz, Ar–H), 8.13 (d, 1H,  $J = 12.0$  Hz, =CH–N), 9.89 (bs, 1H, NH).  $^{13}C$  NMR (50 MHz, DMSO- $d_6$ ):  $\delta = 12.52, 47.00, 99.50, 117.66, 123.53, 126.60, 127.03, 127.47, 128.86, 139.67, 140.42, 148.55, 153.05, 165.16$ . IR (KBr disc,  $cm^{-1}$ ): 3446, 3283, 1662, 1621, 1593, 1553, 1499, 1308, 1286, 1254, 758, 701, 693. Anal. Calcd for  $C_{16}H_{15}N_3OS$  (297.38 g/mol): C, 64.62; H, 5.08; N, 14.13; S, 10.78. Found: C, 64.90; H, 5.09; N, 14.15; S, 10.83.

2.2.9. 3-Methyl-1-phenyl-4-[[pyridin-2-ylmethyl]amino]methylidene]-4,5-dihydro-1H-pyrazol-5-one (**3i**)

0.28 g (63%); white crystals; Mp = 92–93 °C (dec).  $^1H$  NMR (200 MHz, DMSO- $d_6$ ):  $\delta = 2.18$  (s, 3H,  $CH_3$ ), 4.68 (s, 2H,  $CH_2$ ), 7.07 (t, 1H,  $J = 7.4$  Hz, Ar–H), 7.35 (t, 2H,  $J = 7.4$  Hz, Ar–H), 7.42 (two d, 1H,  $J = 4.8$  and 5.8 Hz, Py–H), 7.82 (dt, 1H,  $J = 5.8$  and 1.6 Hz, Py–H), 7.98 (dd, 2H,  $J = 7.4$  and 1.2 Hz, Ar–H), 8.17 (d, 1H,  $J = 8.2$  Hz, =CH–N), 8.54 (dd, 1H,  $J = 4.8$  and 1.6 Hz, Py–H), 8.62 (d, 1H,  $J = 1.6$  Hz, Py–H), 9.90 (bs, 1H, NH).  $^{13}C$  NMR (50 MHz, DMSO- $d_6$ ):  $\delta = 12.57, 50.09, 99.57, 117.65, 123.50, 123.95, 128.86, 133.75, 135.78, 139.73, 148.66, 149.23, 149.40, 153.68, 165.16$ . IR (KBr disc,  $cm^{-1}$ ): 3422, 3205, 1668, 1628, 1593, 1547, 1500, 1488, 1440, 1345, 1238, 759. Anal. Calcd for  $C_{17}H_{16}N_4O$  (292.34 g/mol): C, 69.85; H, 5.52; N, 19.16. Found: C, 70.01; H, 5.54; N, 19.21.

2.2.10. 4-[[Furan-2-ylmethyl]amino]methylidene]-3-methyl-1-phenyl-4,5-dihydro-1H-pyrazol-5-one (**3j**)

0.16 g (38%); yellow-orange powder; Mp = 110–111 °C.  $^1H$  NMR (200 MHz, DMSO- $d_6$ ):  $\delta = 2.17$  (s, 3H,  $CH_3$ ), 4.67 (s, 2H,  $CH_2$ ), 6.42–6.48 (m, 2H, Fur–H), 7.08 (t, 1H,  $J = 7.4$  Hz, Ar–H), 7.36 (t, 2H,  $J = 7.4$  Hz, Ar–H), 7.68 (dd, 1H,  $J = 2.6$  and 1.0 Hz, Fur–H), 7.96 (dd, 2H,  $J = 7.4$  and 1.2 Hz, Ar–H), 8.10 (d, 1H,  $J = 8.8$  Hz, =CH–N), 9.75 (bs, 1H, NH).  $^{13}C$  NMR (50 MHz, DMSO- $d_6$ ):  $\delta = 12.50, 45.24, 99.56, 108.65, 110.97, 117.67, 123.55, 128.86, 139.65, 143.53, 148.51, 150.72, 153.44, 165.20$ . IR (KBr disc,  $cm^{-1}$ ): 3436, 3290, 1666, 1625, 1593, 1502, 1487, 1310, 1299, 761. Anal. Calcd for  $C_{16}H_{15}N_3O_2$  (281.31 g/mol): C, 68.31; H, 5.37; N, 14.94. Found: C, 68.67; H, 5.38; N, 14.97.

2.2.11. 3-Methyl-1-phenyl-4-thioureidomethylidene-4,5-dihydro-1H-pyrazol-5-one (**3k**)

0.30 g (77%); yellow powder; Mp = 227–228 °C (dec).  $^1H$  NMR (200 MHz, DMSO- $d_6$ ):  $\delta = 2.25$  (s, 3H,  $CH_3$ ), 7.16 (t, 1H,  $J = 7.4$  Hz, Ar–H), 7.42 (t, 2H,  $J = 7.4$  Hz, Ar–H), 7.92 (dd, 2H,  $J = 7.4$  and 1.2 Hz, Ar–H), 8.63 (bs, 1H, =CH–N), 9.38 (s, 1H, C(=S)NH), 9.55

(s, 1H, C(=S)NH), 11.44 (bs, 1H, NH).  $^{13}C$  NMR (50 MHz, DMSO- $d_6$ ):  $\delta = 12.59, 106.37, 118.00, 124.55, 129.14, 138.69, 144.01, 150.06, 164.02, 181.66$ . IR (KBr disc,  $cm^{-1}$ ): 3438, 3358, 3319, 3178, 1671, 1633, 1608, 1597, 1498, 1233, 1163, 1004, 756. Anal. Calcd for  $C_{12}H_{12}N_4OS$  (260.32 g/mol): C, 55.37; H, 4.65; N, 21.52; S, 12.32. Found: C, 55.49; H, 4.65; N, 21.53; S, 12.37.

2.2.12. 4-[[4-Methoxy-5-methyl-1H-pyrazol-3-yl]amino]methylidene]-3-methyl-1-phenyl-4,5-dihydro-1H-pyrazol-5-one (**3l**)

0.36 g (74%); yellow powder; Mp = 274–275 °C (dec).  $^1H$  NMR (200 MHz, DMSO- $d_6$ ):  $\delta = 2.27$  (s, 3H,  $CH_3$ ), 2.45 (s, 3H,  $CH_3$ ), 2.56 (s, 3H,  $CH_3$ ), 7.14 (t, 1H,  $J = 7.4$  Hz, Ar–H), 7.41 (t, 2H,  $J = 7.4$  Hz, Ar–H), 7.98 (dd, 2H,  $J = 7.4$  and 1.2 Hz, Ar–H), 8.43 (d, 1H,  $J = 12.6$  Hz, =CH–N), 12.40 (d, 1H,  $J = 12.6$  Hz, NH), 13.11 (s, 1H, NH, Pz).  $^{13}C$  NMR (50 MHz, DMSO- $d_6$ ):  $\delta = 12.48, 12.66, 29.66, 103.43, 108.10, 117.83, 124.04, 129.01, 139.16, 142.35, 144.24, 149.06, 149.23, 164.78, 193.88$ . IR (KBr disc,  $cm^{-1}$ ): 3444, 3254, 1674, 1644, 1619, 1593, 1535, 1494, 1321, 1271, 951, 584. Anal. Calcd for  $C_{17}H_{17}N_5O_2$  (323.35 g/mol): C, 63.15; H, 5.30; N, 21.66. Found: C, 63.20; H, 5.31; N, 21.69.

2.2.13. 4-[[4-Ethoxycarbonyl-1H-pyrazol-3-yl]amino]methylidene]-3-methyl-1-phenyl-4,5-dihydro-1H-pyrazol-5-one (**3m**)

0.33 g (65%); yellow crystals; Mp = 244–245 °C (dec).  $^1H$  NMR (200 MHz, DMSO- $d_6$ ):  $\delta = 1.36$  (t, 3H,  $J = 7.2$  Hz,  $CH_3$ ), 2.54 (s, 3H,  $CH_3$ ), 4.32 (q, 2H,  $J = 7.2$  Hz,  $CH_2$ ), 7.13 (t, 1H,  $J = 7.4$  Hz, Ar–H), 7.41 (t, 2H,  $J = 7.4$  Hz, Ar–H), 7.98 (dd, 2H,  $J = 7.4$  and 1.2 Hz, Ar–H), 8.38 (d, 1H,  $J = 1.8$  Hz, Pz–H), 8.44 (d, 1H,  $J = 12.2$  Hz, =CH–N), 11.78 (d, 1H,  $J = 12.2$  Hz, NH), 13.45 (s, 1H, NH, Pz).  $^{13}C$  NMR (50 MHz, DMSO- $d_6$ ):  $\delta = 12.58, 14.33, 60.42, 101.11, 103.42, 117.87, 124.08, 128.99, 134.10, 139.10, 142.78, 147.96, 149.16, 162.79, 165.10$ . IR (KBr disc,  $cm^{-1}$ ): 3439, 3352, 1661, 1611, 1601, 1541, 1279, 1089, 751. Anal. Calcd for  $C_{17}H_{17}N_5O_3$  (339.35 g/mol): C, 60.17; H, 5.05; N, 20.64. Found: C, 60.28; H, 5.02; N, 20.64.

2.2.14. 4-[[5-(Furan-2-yl)-1H-pyrazol-3-yl]amino]methylidene]-3-methyl-1-phenyl-4,5-dihydro-1H-pyrazol-5-one (**3n**)

0.35 g (70%); yellow crystals; Mp = 230–231 °C (dec).  $^1H$  NMR (200 MHz, DMSO- $d_6$ ):  $\delta = 2.27$  (s, 3H,  $CH_3$ ), 6.65 (two d, 1H,  $J = 2.0$  and 1.6 Hz, Fur–H), 6.79 (d, 1H,  $J = 2.0$  Hz, Fur–H), 6.87 (d, 1H,  $J = 3.2$  Hz, Pz–H), 7.13 (t, 1H,  $J = 7.4$  Hz, Ar–H), 7.41 (t, 2H,  $J = 7.4$  Hz, Ar–H), 7.82 (d, 1H,  $J = 1.6$  Hz, Fur–H), 7.99 (dd, 2H,  $J = 7.4$  and 1.2 Hz, Ar–H), 8.49 (s, 1H, =CH=N), 11.18 (bs, 1H, OH), 13.29 (d, 1H,  $J = 2.0$  Hz, NH, Pz).  $^{13}C$  NMR (50 MHz, DMSO- $d_6$ ):  $\delta = 12.64, 90.91, 101.83, 107.69, 112.12, 117.90, 124.03, 129.00, 135.68, 139.26, 143.67, 144.34, 145.70, 149.13, 149.23, 165.13$ . IR (KBr disc,  $cm^{-1}$ ): 3446, 3231, 1671, 1614, 1596, 1542, 1498, 1400, 1320, 753. Anal. Calcd for  $C_{18}H_{15}N_5O_2$  (333.35 g/mol): C, 64.86; H, 4.54; N, 21.01. Found: C, 65.00; H, 4.86; N, 21.07.

2.2.15. 3-Methyl-4-[[5-methyl-1H-pyrazol-3-yl]amino]methylidene]-1-phenyl-4,5-dihydro-1H-pyrazol-5-one (**3o**)

0.26 g (62%); yellow powder; Mp = 213–214 °C (dec).  $^1H$  NMR (200 MHz, DMSO- $d_6$ ):  $\delta = 2.24$  (s, 3H,  $CH_3$ ), 2.25 (s, 3H,  $CH_3$ ), 6.25 (d, 1H,  $J = 1.4$  Hz, Pz–H), 7.12 (t, 1H,  $J = 7.4$  Hz, Ar–H), 7.40 (t, 2H,  $J = 7.4$  Hz, Ar–H), 7.98 (dd, 2H,  $J = 7.4$  and 1.2 Hz, Ar–H), 8.39 (s, 1H, =CH=N), 11.17 (bs, 1H, OH), 12.45 (s, 1H, NH, Pz).  $^{13}C$  NMR (50 MHz, DMSO- $d_6$ ):  $\delta = 10.82, 12.62, 93.31, 101.35, 117.89, 123.97, 128.98, 139.32, 140.88, 145.64, 148.44, 149.02, 165.18$ . IR (KBr disc,  $cm^{-1}$ ): 3437, 3245, 1669, 1620, 1595, 1548, 1499, 1320, 1302, 755. Anal. Calcd for  $C_{15}H_{15}N_5O$  (281.32 g/mol): C, 64.04; H, 5.37; N, 24.89. Found: C, 64.44; H, 5.40; N, 24.94.

#### 2.2.16. 3-Methyl-1-phenyl-4-[[*(1H-pyrazol-3-yl)amino*]methylidene]-4,5-dihydro-1*H*-pyrazol-5-one (**3p**)

0.36 g (90%); yellow crystals; Mp = 221–222 °C (dec). <sup>1</sup>H NMR (200 MHz, DMSO-*d*<sub>6</sub>): δ = 2.26 (s, 3H, CH<sub>3</sub>), 6.51 (t, 1H, *J* = 2.2 Hz, Pz–H), 7.13 (t, 1H, *J* = 7.4 Hz, Ar–H), 7.40 (t, 2H, *J* = 7.4 Hz, Ar–H), 7.78 (t, 1H, *J* = 2.2 Hz, Pz–H), 7.98 (dd, 2H, *J* = 7.4 and 1.2 Hz, Ar–H), 8.46 (s, 1H, –CH=N), 11.40 (bs, 1H, OH), 12.77 (s, 1H, NH, Pz). <sup>13</sup>C NMR (50 MHz, DMSO-*d*<sub>6</sub>): δ = 12.65, 94.14, 101.48, 117.89, 123.99, 128.99, 131.05, 139.29, 145.86, 148.40, 149.06, 165.17. IR (KBr disc, cm<sup>-1</sup>): 3446, 3215, 1658, 1605, 1551, 1499, 1484, 1285, 756. Anal. Calcd for C<sub>14</sub>H<sub>13</sub>N<sub>5</sub>O (267.29 g/mol): C, 62.91; H, 4.90; N, 26.20. Found: C, 62.98; H, 4.93; N, 26.21.

#### 2.2.17. 3-Methyl-1-phenyl-4-[[*(5-phenyl-1H-pyrazol-3-yl)amino*]methylidene]-4,5-dihydro-1*H*-pyrazol-5-one (**3q**)

0.47 g (91%); yellow crystals; Mp = 263–264 °C (dec). <sup>1</sup>H NMR (200 MHz, DMSO-*d*<sub>6</sub>): δ = 2.28 (s, 3H, CH<sub>3</sub>), 6.95 (d, 1H, *J* = 1.8 Hz, Pz–H), 7.13 (t, 1H, *J* = 7.4 Hz, Ar–H), 7.37–7.54 (m, 5H, Ar–H), 7.75 (dd, 2H, *J* = 7.0 and 1.4 Hz, Ar–H), 8.00 (dd, 2H, *J* = 7.4 and 1.2 Hz, Ar–H), 8.49 (s, 1H, –CH=N), 11.19 (bs, 1H, OH), 13.26 (s, 1H, NH, Pz). <sup>13</sup>C NMR (50 MHz, DMSO-*d*<sub>6</sub>): δ = 12.66, 91.65, 101.73, 117.92, 124.03, 124.06, 125.40, 129.00, 129.02, 129.36, 139.27, 144.18, 145.72, 149.06, 149.29, 165.21. IR (KBr disc, cm<sup>-1</sup>): 3445, 3238, 1671, 1615, 1595, 1550, 1498, 1482, 1404, 1321, 743. Anal. Calcd for C<sub>20</sub>H<sub>17</sub>N<sub>5</sub>O (343.39 g/mol): C, 69.96; H, 4.99; N, 20.39. Found: C, 70.10; H, 5.03; N, 20.44.

### 2.3. Treatment of tumor cell lines

Stock solutions (10 mM) of compounds were made in dimethylsulfoxide (DMSO), and dissolved in corresponding medium to the required working concentrations. Human cervix adenocarcinoma HeLa cells, human chronic myelogenous leukemia K562, human breast cancer MDA-MB-361 and MDA-MB-453 cells and human colon carcinoma LS174 cells were cultured as a monolayer, while were grown in a suspension in the complete nutrient medium, at 37 °C in humidified air atmosphere with 5% CO<sub>2</sub>. For the growth of MDA-MB-361 and MDA-MB-453 cells complete medium was enriched with 1.11 g/L glucose. Neoplastic HeLa cells (2000 cells per well), MDA-MB-361 cells (7000 cells per well), MDA-MB-453 cells (3000 cells per well), human colon carcinoma LS174 cells (7000 cells per well), were seeded into 96-well microtiter plates. Twenty-four hours later, after the cell adherence, five different, double diluted, concentrations of investigated compounds were added to the wells, except for the control cells to which a nutrient medium only was added. K562 cells (3000 cells per well) were seeded, 2 h before addition of investigated compounds to give the desired final concentrations. Nutrient medium was RPMI-1640, supplemented with L-glutamine (3 mM), streptomycin (100 Iu/mL), and penicillin (100 Iu/mL), 10% heat inactivated (56 °C) FBS and 25 mM Hepes, and the pH of the medium was adjusted to 7.2 by bicarbonate solution. The cultures were incubated for 72 h. At the end of this incubation period, antiproliferative activity *in vitro* was determined by the MTT test [12] modified by Ohno and Abe [13]. Results are presented as the mean ± SD of three independent experiments. IC<sub>50</sub> is used as the measure of the toxic agents action and is determined from the graph S(%) = f(c), as the concentration of the agent which induces decrease in cell survival to 50%.

### 2.4. QSAR analysis

The set of 18 compounds synthesized in this study, including edaravone, (Scheme 1) was used for QSAR (quantitative structure–activity relationships) analysis. All structures were constructed using Spartan software [14]. Geometry optimization

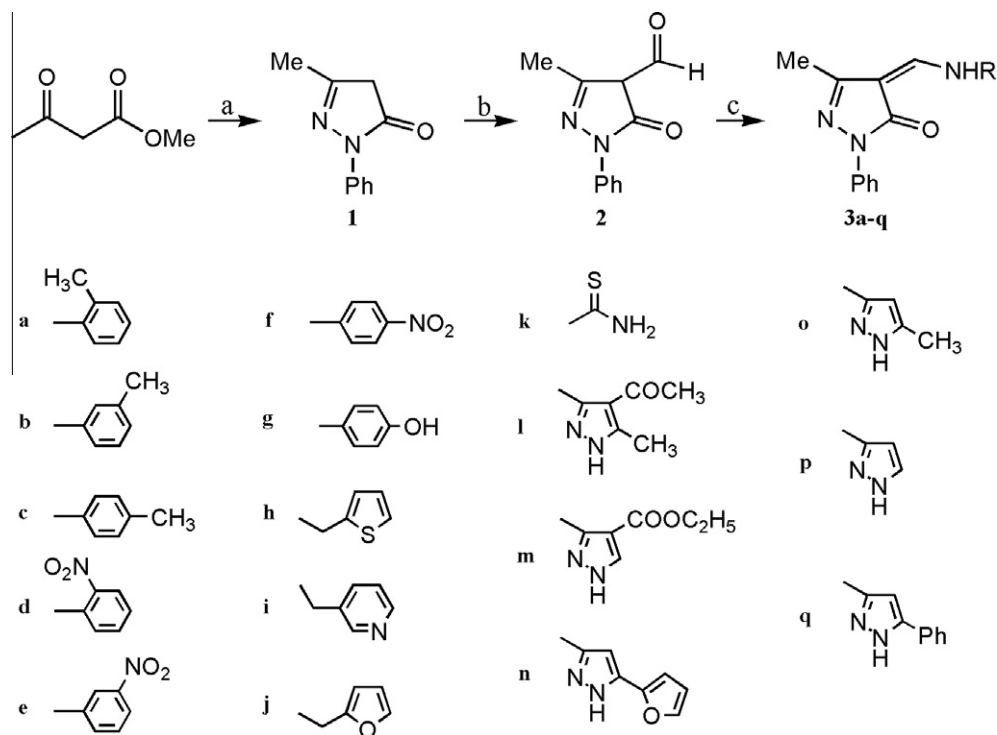
was performed by the AM1 semi-empirical method implemented in the Spartan software. Calculation of descriptors was performed using Codessa software (Comprehensive Descriptors for Structural and Statistical Analysis) [15]. A total of 450 descriptors were calculated and divided into five groups: constitutional, topological, geometrical, electrostatic and quantum-chemical. The heuristic method (HM) implemented in Codessa software was used for the selection of the most significant descriptors for antiproliferative activity of investigated edaravone derivatives on HeLa, MDA-MB-453 and K562 cancer cells. HM, as an advanced algorithm based on MLR, is suitable for preliminary studies of structural features important for activity of ligands, when mechanism of action of new compounds is not discovered yet. The advantage of HM is based on its unique strategy of selecting descriptors on the basis of their statistical significance: (a) first of all, all descriptors are checked to ensure that values of each descriptor are available for each structure, otherwise descriptors for which values are not available in data set are discarded; (b) descriptors having constant value for all structures in the data set are also discarded; (c) thereafter all possible one-parameter regression models are tested and insignificant descriptors are removed; (d) the program calculates the pair correlation matrix of descriptors and further reduces the descriptor pool by eliminating highly correlated descriptors. Therefore, HM represents an excellent tool for descriptor selection in preliminary analysis of structural features affecting the activity of drugs [16]. In this work, we first performed one-parameter heuristic analysis in order to investigate the structural features that are most significant for antitumor activity of compounds synthesized. Then we used heuristic 3-parameter analysis to establish preliminary QSAR equations for antiproliferative activity on HeLa, MDA-MB-453 and K562 cells tested in this study (Table 1).

## 3. Results and discussion

### 3.1. Synthesis and spectral characterization

Compounds **3a–q** were prepared according to Scheme 1. Edaravone **1** was synthesized by the known condensation reaction of β-keto esters with phenylhydrazine. Under Vilsmeier conditions with POCl<sub>3</sub> and *N,N*-dimethylformamide, edaravone **1** was transformed into formylated derivative **2** [17]. Aldehyde precursor **2** was then reacted with selected primary amines affording the desired aminomethylidene derivatives of 4-formylederavone **3a–q** in good to excellent yields.

The preparation of the sufficiently pure aminomethylidene derivatives of 4-formylederavone was not possible by simple classical condensation reaction between aldehyde and amine in an equimolar ratio or in a slight excess of one of the reactants. Namely, the existence of four tautomeric forms of 4-formylederavone **2** [18] can make some difficulties in preparation of 4-aminomethylidene derivatives **3a–q** in high yields and without further purification. Initially, we tried the reaction of aldehyde **2** with primary amine in the presence of a slight excess of amine reagent (10%) but the major product was contaminated with hydroxymethylene tautomer of starting aldehyde. When we carried out this reaction with amines in form of their hydrochloride salts, we found a large content of hydroxymethylene tautomer and very low yield of the final product. Then, we investigated the reaction in the alkaline conditions using 1 equivalent of LiOH and a solid was subjected to column chromatography in order to obtain the pure compound **3**. However, when we performed this reaction with two equivalents of primary amines in the presence of catalytic amount of *p*-toluenesulphonic acid (*p*-TSA), pure compounds were isolated in good to high yields without presence of any



**Scheme 1.** Reagents and conditions: (a) PhNHNH<sub>2</sub>, EtOH, reflux, 3 h; (b) DMF, POCl<sub>3</sub>, heat, 80 °C, 1.5 h; (c) RNH<sub>2</sub>, p-TSA, EtOH, reflux, 2 h.

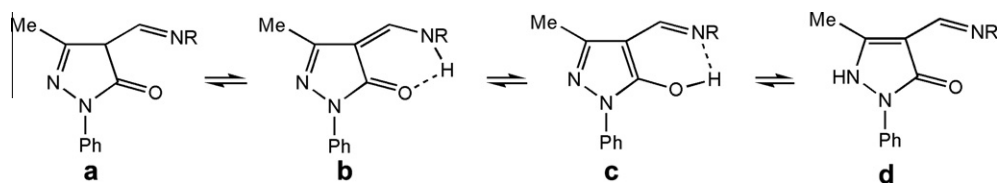
**Table 1**

IC<sub>50</sub> (μg/ml) for the 72 h of action of investigated compounds and cisplatin on the HeLa, MDA-MB-361, MDA-MB-453, K562 and LS174 cells determined by MTT test.

Compounds	HeLa	MDA-MB-361	MDA-MB-453	K562	LS174
IC <sub>50</sub> (μM) <sup>a</sup>					
<b>3a</b>	185.67 ± 0.02	n.d.	>200	154.50 ± 0.96	n.d.
<b>3b</b>	72.91 ± 0.78	n.d.	91.53 ± 0.06	72.79 ± 2.21	n.d.
<b>3c</b>	86.32 ± 0.96	n.d.	>200	137.08 ± 1.65	n.d.
<b>3d</b>	>200	n.d.	169.20 ± 1.76	168.02 ± 1.80	n.d.
<b>3e</b>	183.75 ± 0.21	n.d.	176.74 ± 4.02	115.62 ± 0.93	n.d.
<b>3f</b>	184.15 ± 1.43	n.d.	>200	167.26 ± 1.08	n.d.
<b>3g</b>	180.06 ± 1.11	n.d.	>200	185.15 ± 2.35	n.d.
<b>3h</b>	62.76 ± 0.25	n.d.	110.90 ± 0.53	87.18 ± 1.08	n.d.
<b>3i</b>	148.58 ± 1.84	n.d.	98.18 ± 0.23	80.51 ± 6.24	n.d.
<b>3j</b>	69.18 ± 1.69	n.d.	117.42 ± 1.59	86.82 ± 1.18	n.d.
<b>3k</b>	>200	n.d.	>200	158.92 ± 1.39	n.d.
<b>3l</b>	188.97 ± 0.11	n.d.	178.47 ± 0.43	187.18 ± 0.95	>200
<b>3m</b>	124.10 ± 0.34	n.d.	74.24 ± 0.24	75.65 ± 2.89	88.165 ± 3.55
<b>3n</b>	83.71 ± 1.22	n.d.	44.75 ± 0.12	79.91 ± 0.69	64.825 ± 3.70
<b>3o</b>	130.56 ± 2.23	n.d.	91.06 ± 5.11	79.77 ± 0.65	89.61 ± 1.27
<b>3p</b>	174.19 ± 0.98	n.d.	88.84 ± 1.72	166.39 ± 0.24	126.81 ± 1.44
<b>3q</b>	35.79 ± 2.35	13.63 ± 3.56	10.51 ± 0.09	22.13 ± 3.85	169.48 ± 1.01
<b>Edaravone</b>	195.28 ± 0.33	n.d.	99.36 ± 0.22	108.59 ± 1.35	92.87 ± 5.34
<b>Cis-DDP</b>	2.41 ± 0.14	14.74 ± 0.36	3.75 ± 0.12	7.9 ± 0.20	7.95 ± 0.32

n.d.: Not determined.

<sup>a</sup> Concentrations of examined compounds that induced a 50% decrease in HeLa, MDA-MB-453, K562, and LS174 cell survival (expressed IC<sub>50</sub> (μM)).



**Scheme 2.** Possible tautomers of aminomethylidene derivatives of 4-formylidaravone.

tautomeric form of starting aldehyde or amine reagent. Also, it has been observed that ethanol is the best solvent for carrying out this reaction using p-TSA as an acidic catalyst.

Like aldehyde precursor **2**, aminomethylidene derivatives of 4-formylidaravone **3a–q** can exist in four tautomeric forms (Scheme 2.) in dependence on experimental conditions.

IR spectra of all compounds **3a–q** in KBr disc contain the strong band of the conjugated carbonyl group between 1658 and 1674  $\text{cm}^{-1}$  together with broad absorption band of intramolecularly hydrogen-bonded N–H stretching frequencies at about 3440  $\text{cm}^{-1}$  indicating the tautomer **B** as a main form in the solid state. These observations for N–H stretching frequencies are in accordance with IR spectra of some aminomethylidene derivatives of pyrazol-5-one with exocyclic double bond at C4 position [19]. An X-ray analysis of a similar compound obtained as a condensation product of 4-formyldaravone and 2-aminoethanol confirmed the existence of keto–amine tautomeric form in the solid state [20].

The information obtained from  $^1\text{H}$  NMR spectra in  $\text{DMSO-d}_6$  solution has shown that compounds **3a–m** exist predominantly as **B** structure stabilized by intramolecular hydrogen bonds. A doublet observed as a result of couplings between protons attached to exocyclic carbon atom and amino protons confirms this hypothesis and rules out the presence of other tautomeric structures. Although the splitting of exocyclic CH protons is not well resolved in all homologs, the same structure should exist because it has the same or very similar chemical shift for this proton. Even more, a fast equilibrium change between **B** and **C** tautomers might be present, resulting in appearance of an average NMR signal.

However, 5-substituted-3-aminopyrazole derivatives **3n–q** displayed an intense, sharp singlet for exocyclic CH proton and a strongly deshielded, exchangeable with  $\text{D}_2\text{O}$  signal at the lower field, suggesting the tautomer structure **C** as a dominant form in  $\text{DMSO-d}_6$  solution. This chemical shift value exclude tautomer **D** since in this case, a location of the ring nitrogen proton at significantly higher field should be expected.

### 3.2. Antitumor activity

All synthesized compounds **3a–q** were evaluated for their antiproliferative activity against human cervix adenocarcinoma HeLa cells, human chronic myelogenous leukemia K562, human breast cancer MDA-MB-361 and MDA-MB-453 cells and human colon car-

cinoma LS174 with cisplatin (cis-DDP) as referent cytostatic. Table 1 represents the results of cytotoxic activity, while Fig. 2 depicts the cytotoxic curves from MTT assay showing the survival of MDA-MB-361 and MDA-MB-453 cell grown for 72 h in the presence of increasing concentrations of **3q**.

Tautomerism might play an important role in antitumor activity of all tested compounds against several cell lines. In general, the compounds **3n** and **3q** containing 3-aminopyrazole moiety and existing in tautomeric form **C** showed the most potent antiproliferative activity, especially towards human breast carcinoma cells. Compound **3q** exhibited stronger cytotoxicity in inhibition of MDA-MB-361 type cell lines in comparison with cisplatin. The second important condition for the suppress of cell growth is kind of substituent at C5 position of pyrazole ring from 3-aminopyrazole pharmacophore. It is evident that the heteroaromatic and planar aromatic rings at C5 of pyrazole unit (**3n** and **3q**) more efficiently inhibited the growth of MDA-MB-453 with respective  $\text{IC}_{50}$  value being 2- and 9-fold lower than those observed for the compound **3o** with methyl group at C5 position. Comparing the compounds **3l** and **3m** in the same tautomeric form **B** it has been observed that methyl group at C5 shows a dramatic trend of lowering of cytotoxic activity against all type cell lines. It is interesting to note that edaravone alone was found to be significantly less active than compound **3q**.

### 3.3. QSAR studies

The antiproliferative activity of edaravone against HeLa, MDA-MB-453 and K562 cells occurs even without additional impact of substituent at position C4. The mechanism of direct antiproliferative activity of edaravone on different cancer cells still remains unclear, but it could be supposed that, besides the antioxidant activity for protecting normal cells, edaravone could inhibit hypothetical target that is included in proliferation process of cancer cells. It is noteworthy to emphasize that all our synthesized compounds showed very low antioxidant activity in comparison with edaravone. Regarding the structure of edaravone, possible mode of action with hypothetical target could include H-bond interactions with carbonyl group at position C5 in all possible tautomeric forms, hydrophobic interactions with phenyl ring, as well as interactions with nitrogen in position 2, depending on tautomeric form of edaravone that is predominant in physiological conditions. Introduction of different substituents at position C4 of edaravone increased, more or less significantly, antitumor activity of all derivatives against HeLa cells, and also antitumor activity of some C4-substituted edaravone derivatives against MDA-MB-453 and K562 cells. We tried to investigate the influence of substituents on whole-molecule features of edaravone derivatives, as well as features of substituents as fragments with respect to their antitumor activity, since pyrazolin-5-one core, as well as substituents introduced in position 4, could represent possible pharmacophores for antitumor activity. So we applied heuristic method using whole-molecule descriptors of edaravone derivatives, as well as fragmental descriptors calculated for the substituents, where every substituent at position 4 of edaravone represented one fragment. Variations in antitumor activity of edaravone derivatives have been quantitatively correlated with molecular structure features.

The results of the heuristic method applied on whole-molecule descriptors for activity on HeLa cells are shown in Table 2. The most significant descriptors for antitumor activity on HeLa cells mostly belong to the group of quantum-chemical descriptors, showing that quantum-chemical features of derivatives are the most important for binding to potential target. The most significant descriptor is the average electrophilic reactivity index for C atom, which indicates that electrophilic character of a C atom plays the important role in antitumor activity of investigated compounds on

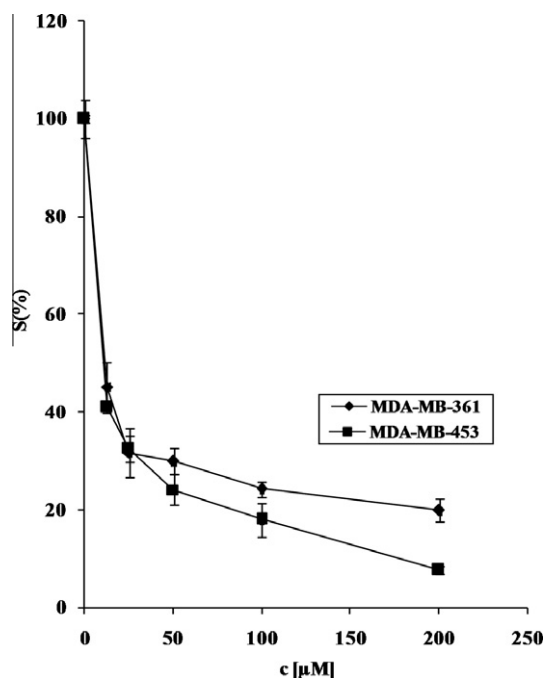


Fig. 2. Representative graph shows survival of MDA-MB-361 and MDA-MB-453 cell grown for 72 h in the presence of increasing concentrations of **3q**.

**Table 2**  
The most significant descriptors of edaravone derivatives for antitumor activity on HeLa cells.

	Descriptor	R <sup>2</sup>	F	Type of feature
1	Average electrophilic reactivity index for a C atom	0.4353	12.33	Quantum-chemical
2	Balaban index	0.4261	11.88	Topological
3	Min. total interaction for a N–N bond	0.3687	9.34	Quantum-chemical
4	Min. e–e repulsion for a N–N bond	0.3626	9.10	Quantum-chemical
5	Number of rings	0.3510	8.65	Constitutional
6	PPSA-1 Partial positive surface area [semi-MO PC]	0.3471	8.51	Quantum-chemical
7	Min. total interaction for a C–H bond	0.3286	7.83	Quantum-chemical
8	Max. n–n repulsion for a C–H bond	0.3262	7.75	Quantum-chemical
9	Min. n–n repulsion for a N–N bond	0.3225	7.62	Quantum-chemical
10	Max. total interaction for a C–H bond	0.3178	7.46	Quantum-chemical

HeLa cells. Less electrophilic C at position 5 of edaravone derivatives determines tautomeric form that is stabilized by intramolecular H-bond and therefore sterically more suitable for binding, whilst possibility of intermolecular H-bond interactions is retained. The electrophilic reactivity index for C atom at position 5 of pyrazolyn-5-one (Eei(C5)) for all compounds was then calculated. The value of Eei(C5) for edaravone is  $10.1 \times 10^{-3}$ , whilst Eei(C5) for compound **3q**, showing highest activity on HeLa cells, is  $0.5 \times 10^{-3}$ . No direct linear correlation was observed for antitumor activity and Eei(C5) for all compounds, but from the values of Eei(C5) for particular compounds it could be concluded that less electrophilic C on position 5 favors tautomeric form **C** that is stabilized by intramolecular H-bonds, providing bioactive geometry of compound required for interaction with binding site, where formation of intermolecular H-bonds with hypothetical active site is still possible. The Number of rings, as constitutional descriptor, also appears to have an influence on binding. It is likely that active site of possible target possesses more than one binding site, therefore number of rings could be important for fitting in hydrophobic pocket. Partial positive surface area might be important for polar interactions with possible polar binding site of the target. The example of such type of active site is exactly Cdc25B phosphatase as target for 3-methyl-4-(O-methyl-oximino)-1-phenylpyrazolin-5-one [21]. Topological descriptors describing the atoms connectivity are also significant for antitumor activity. Balaban index was well correlated with antitumor activity on HeLa cells ( $R^2 = 0.4261$ ).

Applying 3-parameter correlation (the maximal number of descriptors in equation should not exceed 3, regarding the number of compounds), following QSAR equation for antitumor activity on HeLa cells has been obtained:

$$\log(1/IC50(\text{HeLa})) = 1.4772 \cdot E_{\text{tot}}(\text{CH}) + 48.0430 \cdot V_{\text{C}}^{\text{max}} - 36.0390 \cdot \text{Eni}^{\text{min}}(\text{O}) - 210.05 \quad (n = 16, R^2 = 0.8542) \quad (1)$$

The descriptors included in Eq. (1) are presented in Table 3, and they all belong to the group of quantum-chemical descriptors, which confirms that quantum-chemical interactions with binding site are most important for antitumor activity on HeLa cells. Increasing the maximum total interaction for a C–H bond, and decreasing the maximum valency of a C atom and the minimum nucleophilic reactivity index for an O atom can lead to an increase

in cytotoxicity against HeLa. Nucleophilic character of O atom appears to be the most important factor determining cytotoxicity of edaravone derivatives on HeLa cells.

The most significant fragmental descriptors (calculated for every substituent at position 4 of edaravone as fragment) for antitumor activity on HeLa cells are presented in Table 4. The results are in accordance with supposition that there is another binding site at target for interaction of edaravone substituents at position 4. The most significant descriptor is the relative negative charged surface area, indicating polar interactions of substituents with binding site. Other important descriptors belong to the topological and constitutional group. The number of rings also indicates that there is hydrophobic pocket of precise geometry which explains why compound **3q** shows considerably higher cytotoxicity on HeLa cells. Introduction of nitro group in aromatic phenyl ring decreased antitumor activity of compounds **3d**, **3e** and **3f**, probably due to conjugation of nitro group with phenyl ring, resulting in decrease of hydrophobic interactions of phenyl ring and enlargement of the plane area that perhaps could not fit with size of hydrophobic binding site.

The most significant whole-molecule descriptors for antitumor activity on MDA-MB-453 cells obtained by heuristic method are presented in Table 5. Most of the descriptors belong to the group of quantum-chemical descriptors, confirming that cytotoxicities of these compounds appear to be mainly governed by quantum-chemical factors. The Number of rings, as constitutional descriptor, also plays significant role in antitumor activity on MDA-MB-453 cells.

Applying 3-parameter correlation for antitumor activity on MDA-MB-453 cells, following equation has been obtained:

$$\log(1/IC50(\text{MDA-MB-453})) = -158.41 \cdot \text{Eei}^{\text{max}}(\text{O}) + 0.0260 \cdot {}^{\text{q}}\text{HDCA} - 0.8817 \cdot P_{\text{O}}^{\text{avg}} - 0.4107 \quad (n = 13, R^2 = 0.9257) \quad (2)$$

The descriptors included in Eq. (2) are presented in Table 6, and they belong to the group of quantum-chemical descriptors.

Decreasing the electrophilic reactivity index for an O atom and the average bond order of an O atom, and increasing the H-donors charged surface area will increase the cytotoxicity of edaravone derivatives on MDA-MB-453 cells. It appears that H-bonds interac-

**Table 3**  
Descriptors included in Eq. (1).

	Descriptor	Type of feature
1	Max. total interaction for a C–H bond ( $E_{\text{tot}}(\text{CH})$ )	Quantum-chemical
2	Max. valency of a C atom ( $V_{\text{C}}^{\text{max}}$ )	Quantum-chemical
3	Min. nucleophilic reactivity index for a O atom ( $\text{Eni}^{\text{min}}(\text{O})$ )	Quantum-chemical

**Table 4**

The most significant fragmental descriptors for antitumor activity on HeLa cells.

	Fragmental descriptor	R <sup>2</sup>	F	Type of feature
1	f-RNCS relative negative charged SA [semi-MO PC]	0.5080	15.49	Quantum-chemical
2	f-Balaban index	0.4290	11.27	Topological
3	f-FNSA-3 fractional PNSA (PNSA-3/TFSA) [semi-MO PC]	0.3794	9.17	Quantum-chemical
4	f-Max. n–n repulsion for a C–H bond	0.3775	9.09	Quantum-chemical
5	f-Max. total interaction for a C–H bond	0.3333	7.5	Quantum-chemical
6	f-FHBCA fractional HBCA (HBCA/TFSA) [semi-MO PC]	0.3280	7.32	Quantum-chemical
7	f-Max. resonance energy for a C–H bond	0.3177	6.98	Quantum-chemical
8	f-FNSA-3 fractional PNSA (PNSA-3/TMSA) [semi-MO PC]	0.3173	6.97	Quantum-chemical
9	f-PPSA-1 partial positive surface area [semi-MO PC]	0.3155	6.91	Quantum-chemical
10	f-Number of rings	0.3128	6.83	Constitutional

**Table 5**

The most significant descriptors for antitumor activity on MDA-MB-453 cells.

	Descriptor	R <sup>2</sup>	F	Type of feature
1	Max. resonance energy for a C–H bond	0.5522	19.73	Quantum-chemical
2	Max. n–n repulsion for a C–H bond	0.5411	18.87	Quantum-chemical
3	Min. exchange energy for a C–H bond	0.4340	12.27	Quantum-chemical
4	Relative number of rings	0.4207	11.62	Constitutional
5	Average electrophilic reactivity index for a C atom	0.4032	10.81	Quantum-chemical
6	Min. (>0.1) bond order of a C atom	0.3930	10.36	Quantum-chemical
7	Max. exchange energy for a N–N bond	0.3762	9.65	Quantum-chemical
8	Max. total interaction for a C–H bond	0.3732	9.53	Quantum-chemical
9	Max. e–e repulsion for a N–N bond	0.3556	8.83	Quantum-chemical
10	Min. exchange energy for a N–N bond	0.3456	8.45	Quantum-chemical

**Table 6**

Descriptors included in Eq. (2).

	Descriptor	Type of feature
1	Max. electrophilic reactivity index for a O atom (Eei <sup>max</sup> (O))	Quantum-chemical
2	HDCA H-donors charged surface area [semi-MO PC] ( <sup>q</sup> HDCA)	Quantum-chemical
3	Average bond order of a O atom (P <sub>O</sub> <sup>avg</sup> )	Quantum-chemical

**Table 7**

The most significant fragmental descriptors for antitumor activity on MDA-MB-453 cells.

	Fragmental descriptor	R <sup>2</sup>	F	Type of feature
1	f-Max. resonance energy for a C–H bond	0.6591	29.00	Quantum-chemical
2	f-Max. n–n repulsion for a C–H bond	0.6025	22.74	Quantum-chemical
3	f-Max. atomic state energy for a N atom	0.4792	13.80	Quantum-chemical
4	f-Max. exchange energy for a C–N bond	0.4691	13.25	Quantum-chemical
5	f-Average electrophilic reactivity index for a N atom	0.4647	13.02	Quantum-chemical
6	f-Average Information content (order 2)	0.4480	12.18	Topological
7	f-Number of rings	0.4259	11.13	Constitutional
8	f-Min. exchange energy for a C–H bond	0.4248	11.08	Quantum-chemical
9	f-Balaban index	0.4177	10.76	Topological
10	Max. coulombic interaction for a H–N bond	0.4176	10.77	Quantum-chemical

tions are most important for cytotoxicity of edaravone derivatives on MDA-MB-453 cells.

The most significant fragmental descriptors for antitumor activity on MDA-MB-453 are presented in Table 7. They belong to the group of quantum-chemical, topological and constitutional descriptors. The results suggest existence of hydrophobic pocket at binding site that is supposed to interact with certain substituents of edaravone derivatives increasing their antitumor activity on MDA-MB-453 cells.

The most significant whole-molecule descriptors for antitumor activity on K562 cells are presented in Table 8. They belong to quantum-chemical and electrostatic descriptors. It indicates that polar interactions of edaravone derivatives with target in K562 cells are important for the antitumor activity.

Applying 3-parameter correlation for antitumor activity on K562 cells, following equation has been obtained:

$$\log(1/IC50(K562)) = -119.51 \cdot Eei^{avg}(O) + 28.24 \cdot Eni^{min}(O) - 0.1486 \cdot {}^qRPCS - 1.4633$$

$$(n = 18, R^2 = 0.7458) \quad (3)$$

The descriptors included in Eq. (3) are presented in Table 9, and they belong to the group of quantum-chemical and electrostatic descriptors.

Decreasing the average electrophilic index for an O atom and the relative positive charged surface area, and increasing the minimal nucleophilic reactivity index for an O atom the cytotoxicity of the edaravone derivatives on K562 cells should increase.

**Table 8**  
The most significant descriptors for antitumor activity on K562 cells.

	Descriptor	$R^2$	$F$	Type of feature
1	Average electrophilic reactivity index for a C atom	0.3352	8.07	Quantum-chemical
2	Max. resonance energy for a C–H bond	0.2890	6.50	Quantum-chemical
3	Max. n–n repulsion for a C–H bond	0.2859	6.41	Quantum-chemical
4	FNSA-3 Fractional PNSA (PNSA-3/TMSA) [semi-MO PC]	0.2296	4.77	Quantum-chemical
5	Min. exchange energy for a N–N bond	0.2243	4.63	Quantum-chemical
6	Min. total interaction for a C–H bond	0.2213	4.55	Quantum-chemical
7	Average electrophilic reactivity index for a O atom	0.2161	4.41	Quantum-chemical
8	Max. total interaction for a C–H bond	0.2080	4.20	Quantum-chemical
9	Min. total interaction for a N–N bond	0.1966	3.92	Quantum-chemical
10	RPCS relative positive charged SA (SAMPOS * RPCG) [Zefirov's PC]	0.1964	3.91	Electrostatic

**Table 9**  
Descriptors included in Eq. (3).

	Descriptor	Type of feature
1	Average electrophilic reactivity index for a O atom ( $E_{\text{ej}}^{\text{av}}(\text{O})$ )	Quantum-chemical
2	Min. nucleophilic reactivity index for a O atom ( $E_{\text{n}}^{\text{min}}(\text{O})$ )	Quantum-chemical
3	RPCS relative positive charged SA (SAMPOS * RPCG) [Zefirov's PC] ( $^{\text{e}}\text{RPCS}$ )	Electrostatic

**Table 10**  
The most significant fragmental descriptors for antitumor activity on K562 cells.

	Fragmental descriptor	$R^2$	$F$	Type of feature
1	f-Max. n–n repulsion for a C–H bond	0.3972	9.88	Quantum-chemical
2	f-Max. resonance energy for a C–H bond	0.3806	9.22	Quantum-chemical
3	f-WPSA-1 weighted PPSA (PPSA1 * TFSA/1000) [semi-MO PC]	0.3545	8.24	Quantum-chemical
4	f-Balaban index	0.3519	8.14	Topological
5	f-RNCS relative negative charged SA (SAMNEG * RNCG) [semi-MO PC]	0.3358	7.58	Quantum-chemical
6	f-Structural information content (order 2)	0.3115	6.79	Topological
7	f-WPSA-1 weighted PPSA (PPSA1 * TMSA/1000) [semi-MO PC]	0.3017	6.48	Quantum-chemical
8	f-Average information content (order 2)	0.2922	6.19	Topological
9	f-Average electrophilic reactivity index for a N atom	0.2858	6.00	Quantum-chemical
10	f-PPSA-1 partial positive surface area [semi-MO PC]	0.2834	5.93	Quantum-chemical

These preliminary QSAR equations for antitumor activity of edaravone derivatives on HeLa, MDA-MB-453 and K562 cells give us insight about the importance of quantum-chemical and electrostatic factors for the prediction of cytotoxicity. It is clear that electrophilic/nucleophilic ratio of O atom as well as polar surface areas play very important role in antitumor activity of derivatives investigated. Further investigation, including more derivatives and detailed study of the particular fragments and atoms and their effects, could possibly provide reliable model for the prediction of cytotoxicity of these derivatives.

The most significant fragmental descriptors for antitumor activity on K562 cells are presented in Table 10. They belong to the group of quantum-chemical and topological descriptors. The differences in selected descriptors comparing to those presented for antitumor activity on HeLa and MDA-MB-453 suggest that interaction of compounds with binding site on K562 cells partially differ in nature and strength. From the descriptors presented in Table 10, it could be supposed that another interaction occurs with nitrogen at position 2 of edaravone. The target for these agents could be the same or similar for all three types of cancer cells, but some differences in cells intracellular environment may influence formation of predominant tautomeric form of compounds. Stronger interactions of basic pyrazolin-5-one core with target in K562 cells, possibly due to additional interactions with nitrogen at position 2, could be possible explanation why all structures investigated show some activity on K562 cells, no matter of substituent introduced. Also, it appears that polar interactions are the most important for antitumor activity on K562 cells.

Correlation of lipophilicity parameter  $\log P$  with antitumor activity of edaravone derivatives on HeLa, MDA-MB-453 and K562 did not give significant results ( $r^2 = 0.1858$ ,  $r^2 = 0.0006$  and

$r^2 = 0.0466$  for antitumor activity on HeLa, MDA-MB-453 and K562, respectively), perhaps because the range of  $\log P$  in this congeneric set was not statistically representative. It remains to be additionally investigated whether lipophilicity plays an important role in antitumor activity, as well as transport to cells of edaravone derivatives, by variation of lipophilic and hydrophilic substituents.

The action mechanism of investigated cytotoxic compounds still remains complicated since there are many factors that may influence activity of these agents. Here, we just offer some theoretical considerations based on the QSAR heuristic approach expecting that this results might give some guidance for further design and improvement of antitumor activity of related derivatives. It is interesting that cytotoxicities of these compounds against all three type of cells investigated appear to be mainly governed by quantum-chemical factors. Besides, it could be concluded that active site for these compounds could be consistent of more than one binding site, and that additional binding sites interact with ligands by hydrophobic and polar interactions, which might give some guidance in searching for target of these potential antitumor compounds.

#### 4. Conclusion

Seventeen structurally different aminomethylidene derivatives of 4-formyledaravone were prepared and characterized using spectroscopic techniques and elemental analysis. Compound **3q** was found to be the most active against human breast cancer MDA-MB-361 and MDA-MB-453 cell lines. In the cell growth inhibition of MDA-MB-361 cells this compound showed a cytotoxic potential practically comparable to cisplatin as referent cytostatic. The most significant fragmental descriptors for antitumor activity on MDA-

MB-453 cells belong to the group of quantum-chemical, topological and constitutional descriptors.

### Acknowledgment

The authors are grateful to the Ministry of Science and Technological Development of the Republic of Serbia for financial support (Grant Nos. 172016 and 145006).

### References

- [1] N. Zhang, M. Komine-Kobayashi, R. Tanaka, M. Liu, Y. Mizuno, T. Urabe, *Stroke* 36 (2005) 2220–2225.
- [2] T. Watanabe, M. Tahara, S. Todo, *Cardiovasc. Ther.* 26 (2008) 101–114.
- [3] K. Sujatha, G. Shanthi, N. Panneer Selvam, S. Manoharan, P.T. Perumal, M. Rajendran, *Bioorg Med. Chem. Lett.* 19 (2009) 4501–4503.
- [4] X. Fan, X. Zhang, L. Zhou, K.A. Keith, E.R. Kern, P.F. Torrence, *Bioorg. Med. Chem. Lett.* 16 (2006) 3224–3228.
- [5] D. Castagnolo, F. Manetti, M. Radi, B. Bechi, M. Pagano, A. De Logu, R. Meleddu, M. Saggi, M. Botta, *Bioorg Med. Chem.* 17 (2009) 5716–5721.
- [6] R. Tripathy, A. Ghose, J. Singh, E.R. Bacon, T.S. Angeles, S.X. Yang, M.S. Albom, L.D. Aimone, J.L. Herman, J.P. Mallamo, *Bioorg. Med. Chem. Lett.* 17 (2007) 1793–1798.
- [7] S. Kokura, N. Yoshida, N. Sakamoto, T. Ishikawa, T. Takagi, H. Higashihara, N. Nakabe, O. Handa, Y. Naito, T. Yoshikawa, *Cancer Lett.* 229 (2005) 223–233.
- [8] T. Arai, M. Nonogawa, K. Makino, N. Endo, H. Mori, T. Miyoshi, K. Yamashita, M. Sasada, M. Kakuyama, K. Fukuda, *J. Pharmacol. Exp. Ther.* 324 (2008) 529–538.
- [9] Y. Kakiuchi, N. Sasaki, M. Satoh-Masuoka, H. Murofushi, K. Murakami-Murofushi, *Biochem. Biophys. Res. Commun.* 320 (2004) 1351–1358.
- [10] P. Pevarello, M.G. Brasca, P. Orsini, G. Traquandi, A. Longo, M. Nesi, F. Orzi, C. Piutti, P. Sansonna, M. Varasi, A. Cameron, A. Vulpetti, F. Roletto, R. Alzani, M. Ciomei, C. Albanese, W. Pastori, A. Marsiglio, E. Pesenti, F. Fiorentini, J.R. Bischoff, C. Mercurio, *J. Med. Chem.* 48 (2005) 2944–2956.
- [11] D. Bebbington, H. Binch, J.D. Charrier, S. Everitt, D. Frayse, J. Golec, D. Kay, R. Knechtel, C. Mak, F. Mazzei, A. Miller, M. Mortimore, M. O' Donnell, S. Patel, F. Pierard, J. Pinder, J. Pollard, S. Ramaya, D. Robinson, A. Rutherford, J. Studley, J. Westcott, *Bioorg. Med. Chem. Lett.* 19 (2009) 3586–3592.
- [12] T. Mosmann, *J. Immunol. Methods* 65 (1983) 55–63.
- [13] M. Ohno, T. Abe, *J. Immunol. Methods* 145 (1991) 199–203.
- [14] Spartan '02 for Linux, Wavefunction, Inc. Irvine, CA, 2002.
- [15] A.R. Katritzky, W.S. Lobanov, M. Karelson Codessa, Reference Manual (version 2.0), Gainesville, FL, 1994, p. 2.
- [16] P. Liu, W.H. Long, *Int. J. Mol. Sci.* 10 (2009) 1978–1998.
- [17] D.J. Wallace, J.M. Straley, *J. Org. Chem.* 26 (1961) 3825–3826.
- [18] A.I. Movchan, A.R. Kurbangaliev, O.N. Kataeva, I.A. Litvinov, G.A. Chmutova, *Russ. J. Gen. Chem.* 73 (2003) 1130–1136.
- [19] J. Belmar, F.R. Pérez, J. Alderete, C. Zúñiga, *J. Braz. Chem. Soc.* 16 (2005) 179–189.
- [20] B.T. Thaker, K.R. Surati, S. Oswal, R.N. Jadeja, V.K. Gupta, *Struct. Chem.* 18 (2007) 295–310.
- [21] K.R. Kim, J.L. Kwon, J.S. Kim, Z. No, H.R. Kim, H.G. Cheon, *Eur. J. Pharmacol.* 528 (2005) 37–42.